A chromosome-level genome assembly of *Neotoxoptera formosana* (Takahashi, 1921) (Hemiptera: Aphididae)

Shuai Ye[1], Chen Zeng[2], Jian-Feng Liu[1*], Chen Wu[3], Yan-Fei Song[1], Yao-Guo Qin[4], Mao-Fa Yang[1,5*]

[1]Institute of Entomology, Guizhou University; Guizhou Provincial Key Laboratory for Agricultural Pest Management of the Mountainous Region; Scientific Observing and Experimental Station of Crop Pest in Guiyang, Ministry of Agriculture, Guiyang, 550025, China

[2]Puding Plant Protection and Quarantine Station, Guizhou, Puding, 562100, China

[3]The New Zealand Institute for Plant and Food Research Limited, Auckland 1142, New Zealand

[4]Department of Entomology and MOA Key Laboratory for Monitoring and Environment-Friendly Control of Crop Pests, College of Plant Protection, China Agricultural University, Beijing 100193, China

[5]College of Tobacco Science, Guizhou University, Guiyang, 550025, China

*Author for Correspondence: jianfengliu25@126.com; gdgdly@126.com

Abstract

Neotoxoptera formosana (Takahashi), the onion aphid, is an oligophagous pest that mainly feeds on plants from the *Allium* genus. It sucks nutrients from the plants and indirectly acts as a vector for plant viruses. This aphid causes severe economic losses to *Allium tuberosum* agriculture in China. To better understand the host plant specificity of *N. formosana* on *Allium* plants and provide essential information for the control of this pest, we generated the entire genome using Pacific Biosciences long-read sequencing and Hi-C data. Six chromosomes were assembled to give a final size of 372.470 Mb, with an N50 scaffold of

66.911 Mb. The final draft genome assembly, from 192 Gb of raw data, was approximately 371.791 Mb in size, with an N50 contig of 24.99 Kb and an N50 scaffold of 2.637 Mb. The average GC content was 30.96%. We identified 73 Mb (31.22%) of repetitive sequences, 14,175 protein-coding genes and 719 non-coding RNAs. The phylogenetic analysis showed that *N. formosana* and *Pentalonia nigronervosa* are sister groups. We found significantly expanded gene families that were involved in the THAP domain, the DDE superfamily endonuclease, zinc finger, immunity (ankyrin repeats), digestive enzyme (Serine carboxypeptidase) and chemosensory receptor. This genome assembly could provide a solid foundation for future studies on the host specificity of *N. formosana* and pesticide resistant aphid management.

Keywords: *Neotoxoptera formosana*, genome assembly, chromosome-level genome, gene family evolution, Hi-C

Significance: Onion aphids cause significant economic losses to *Allium* plant agriculture, particularly *A. tuberosum*. However, there is very little knowledge of this aphid, in terms of genetics. To expand the genetic resource of this pest, we assembled the whole genome and found the expanding gene families of *N. formosana*. This will provide opportunities for future studies on *N. formosana* genetics and will eventually contribute to aphid control.

Introduction

Allium crop species are used worldwide as vegetables and play an important role in daily diets in Asia (Shahrajabia et al. 2020). These *Allium* vegetables contain various sulfur and organic compounds that exhibit anticancer activities and may be useful for the treatment and prevention of cancers (Asemani et al. 2019). During our previous investigation, we found that *Neotoxoptera formosana* (Takahashi) (Hemiptera: Aphididae) causes significant economic

losses to *Allium* plant agriculture, particularly *A. tuberosum*. *Neotoxoptera formosana*, also known as the onion aphid, damages *Allium* plants by sucking the cell sap from the plants, spreading many plant viruses and defecating sticky honeydew (Wang et al. 2021; Lin et al. 2022).

Onion aphids can search for *Allium* plants but show a significant response to the repellent effects of volatile sulfides, which are released by the plants (Horil 2007), and substances such as rosemary (Horil & Komatsu 1997). This aphid survives all year round but there are two main hazard peaks in the year; March-May and July-September, in Guizhou province, China. Previous studies have found that the predatory gall midge, *Aphidoletes aphidimyza,* has a good control efficiency against *N. formosana* under laboratory conditions (Wang et al. 2021). The complete mitochondrial genome of *N. formosana* was sequenced and annotated by Song et al. (2021). Despite its highly specialized host range and significant economic losses to *Allium* plant agriculture, no genome information for *N. formosana* has been published. In this study, we provided a chromosome-level genome assembly of *N. formosana*. This is the first genome assembly of this genus and will provide important basic information for the study of aphid taxonomy, host plant specificity and pesticide resistant aphid management.

Materials and Methods

Sample Collection and Sequencing

The onion aphids used for sequencing were obtained from Puding County, Anshun City, Guizhou Province, China (105° 270 49″ E, 26° 260 36″ N), in December 2020, and were reared in the laboratory at the Institute of Entomology, Guizhou University (Figure 1). There were 90, 30 and 60 adult females used for PacBio sequencing, RNA-Seq analysis

and Hi-C sequencing, respectively. High quality DNA was extracted using the QIAGEN DNeasy Blood and Tissue kit. For PacBio sequencing, a 20 kb insert-size library was constructed using the SMRTbell™ Template Prep Kit 2.0 and sequencing was performed on the PacBio Sequencer Sequel II. For the Illumina sequencing, the Truseq DNA PCR-free kit was used to construct PCR-free libraries with an insert size of 350 bp. For the RNA-Seq analysis, the TRIzol™ Reagent kit was used to extract RNA and libraries were constructed using the TruSeq RNA v2 kit. The Hi-C library construction was performed by Berry Genomics and included cross-linking, restriction enzyme (MboI) digestion, fragment end repair, DNA cyclization and DNA purification. All the Illumina libraries were sequenced on a NovaSeq 6000, to achieve reads of 150 bp in length.

Genome Assembly

The Illumina genomic datasets were assessed for quality and trimmed using BBTools v38.82 (Bushnell 2014), using the following steps: a) the duplicated sequences were removed using clumpify.sh; b) bbduk.sh was used to remove low quality bases (< Q20), sequences shorter than 15 bases and poly-A/G/C tails (longer than 10 bases). It was also used to correct bases from overlapping reads (qtrim = rl, trimq = 20, minlen = 15, ecco = t, maxns = 5, trimpolya = 10, trimpolyg = 10, trimpolyc = 10). The kmer analysis was performed using Genomescope v2.0 (Vurture *et al*. 2017), with the maximum k-mer coverage of 10,000. The kmer frequency was calculated using the khist.sh script from BBTools (kmer length: 21). The PacBio raw long reads that passed quality control were assembled using wtdbg2 v2.5 (Ruan & Li 2020), with the parameters of "-X 300 -p 15 -k 0 -S 4 -e 2". Polishing of the assembly was performed using NextPolish v1.3.1 (Hu *et al*. 2020), with one round of long read polishing and two rounds of short read polishing. For short read polishing, the reads were first mapped to the assembly using minimap2 v2.22

(Li 2018), with default parameters, and the produced ".sam" files were converted to ".bam" using samtools v1.10 (Li *et al*. 2009). The haplotypic duplications were removed from the assembly using Purge_dups v1.2.5 (Guan *et al*. 2020), with "-a 70". To assign contigs to chromosomes, Juicer v1.6.2 (Durand *et al*. 2016) was first used to align the high quality Hi-C reads to the assembly and the contigs were then scaffolded using 3D-DNA v180922 (Dudchenko *et al*. 2017), with default parameters. The generated pre-pseudochromosomes were manually corrected using Juicerbox v1.11.08 (Durand *et al*. 2016), based on the Hi-C contact maps, and the files were then imported into 3D-DNA to produce the final chromosomal assembly. The contaminated sequences were assessed and removed, using MMseqs2 v12-113e3 (Steinegger & Söding 2017), by blasting contigs against the *nt* and UniVec databases. The cleaned assembly was also uploaded to NCBI for an additional search for possible contamination. The assembly completeness was assessed using BUSCO v3.0.2 (Waterhouse *et al*. 2018), with searches against "insect_odb10". To assess the coverage of raw data, the reads were mapped to the assembly using Minimap2 v2.22. To investigate genome collinearity with *Acyrthosiphon pisum* and *Rhopalosiphum maidis*, MMseq2 v12-113e3 was first used to align protein sequences with "blastp", with parameters of "s 7.5 --alignment-mode 3 --num-iterations 4 -e 1e-5 --max-accept 5". The resulting files, together with the annotation file (all.gff), were then used as inputs to MCScanX for collinearity analysis and were visualized using TBtools v1.0692 (Chen *et al*. 2020).

Genome Annotation

We annotated repeats, protein-coding genes and non-coding RNAs from the assembly. To identify repeats, RepeatModeler v2.0.2a (Flynn *et al*. 2020) was first used to generate a *de novo* repeat library with the parameter of "-LTRStruct". This repeat library was then

merged with the sequences from the RepBase-20181026 (Bao *et al*. 2015) database to form a more extensive repeat library, which was used as the input into RepeatMasker v4.1.0 (Smit *et al*. 2013–2015). The protein-coding gene models were predicted using MAKER v3.01.03 (Holt and Yandell 2011), by integrating the predictions from three strategies. EVidenceModeler (EVM) was used for evidence weighting. The three strategies were: 1) *ab initio* prediction: BRAKER v2.1.6 (Hoff *et al*. 2016) was used to train Augustus v3.4.0 (Stanke *et al*. 2004) and GeneMark-ES/ET/EP 4.68_lic (Brůna *et al*. 2020) and then predict genes with the evidence from RNA-Seq data, to improve accuracy. Alignments from the RNA-Seq analysis were generated using HISAT2 v2.2.1 (Kim *et al*. 2019); 2) Transcript-based gene structure prediction: a reference-guided transcriptome assembly was generated using StringTie v2.1.6 (Kovaka *et al*. 2019), by assembling RNA-Seq reads. This assembly was then aligned to the genome assembly using HISAT2; 3) Protein-homology based prediction: the characterized protein sequences from the phylogenetically close species, *Acyrthosiphon pisum*, *Drosophila melanogaster*, *Nilaparvata lugens*, *Thrips palmi*, *Rhopalosiphum maidis* and *Pediculus humanus*, were downloaded from NCBI for the model.

Gene functional annotation was conducted in three steps: 1) gene models were searched against the UniProtKB (SwissProt+TrEMBL) and *nr* databases. To search against UniProtKB, the sensitive mode (--very-sensitive -e 1e-5) was used for Diamond v2.0.11.149 (Buchfink *et al*. 2015) to obtain functional description; 2) gene models were searched against the Pfam, Smart, Superfamily and CDD databases using InterProScan 5.48-83.0 (Quevillon *et al*. 2005) and the eggNOG v5.0 (Huerta-Cepas *et al*. 2019) database, with eggNOG-mapper v2.1.5 (Huerta-Cepas *et al*. 2017). These data were used to predict protein domains, gene ontology (GO) terms, KEGG and Reactome pathways; 3) The results generated from the above were integrated to produce the final functional

annotation.

To annotate non-coding RNAs, infernal v1.1.4 was used to annotate rRNA, snRNA and miRNA by searching against the Rfam database. The tRNAs were annotated using tRNAscan-SE v2.0.9 (Chan and Lowe 2019) and the predicted tRNAs with low fidelity were removed with the "EukHighConfidenceFilter" script.

Species phylogeny and gene family evolution

We downloaded protein sequences from 15 species from NCBI to infer gene family homology. These species covered orders, tribes and families and included *Thrips palmi*, *Acyrthosiphon pisum*, *Sitobion miscanthi*, *Diuraphis noxia*, and *Myzus persicae*, *Aphis gossypii*, *Melanaphis sacchari, Pentalonia nigronervosa*, *Rhopalosiphum maidis*, *Eriosoma lanigerum*, *Sipha flava*, *Nilaparvata lugens*, *Phenacoccus solenopsis*, *Riptortus pedestris* and *Pachypsylla venusta*. The sequences were initially clustered using OrthoFinder v2.3.8 (Emms and Kelly 2019) and then aligned using Diamond. To generate alignments for species phylogenetic tree construction, the 1,273 single-copy gene clusters were aligned individually to generate homologous regions using MAFFT v7.453 (Katoh and Standley 2013), with "L-INS-I". The regions that were inappropriately aligned were trimmed using trimAl v1.4.1. To construct the phylogeny, FASconCAT-G v1.04 (Kück and Longo 2014) was used to generate a supermatrix as the input for IQ-TREE v2.1.3 (Minh *et al*. 2020), with settings of "--symtest-remove-bad --symtest-pval 0.10 --m MFP --mset LG --msub nuclear --rclusterf 10 --B 1000 --alrt 1000".

The estimation of evolutionary time because species divergence was performed using MCMCTREE, from the PAML v4.9j package, with parameters of "clock = 2, RootAge = < 3.827, model = 0, BDparas = 1 1 0.1, kappa_gamma = 6 2, alpha_gamma = 1 1, rgene_gamma = 2 20 1, sigma2_gamma = 1 10 1". There were six sets of fossil evidence

downloaded from the PBDB database (https://www.paleobiodb.org/navigator/) and used as calibrations for this estimation: Hemiptera and Thysanoptera (<3.827 Mya) as the root, Sternorrhyncha (3.146-3.589 Mya), Aphalaridae and Pseudococcidae (2.793-3.232 Mya), Aphididae (0.996-1.4 Mya), Macrosiphini (>0.339 Mya) and *Nilaparvata lugens* and *Riptortus pedestris* (2.989-3.232 Mya).

The prediction of gene family expansion and contraction within *N. formosana*, when compared with the other 15 species, was conducted using CAFÉ v4.2.1, with the model of single birth-death parameter lambda and a significance level of 0.01 ($p = 0.01$). The significantly expanded/contracted gene families were then assigned to GO and KEGG categories, using R package clusterProfiler v3.10.1 (Yu et al. 2012), with the default parameters ($p = 0.01$ and $q = 0.05$).

Results and Discussion

Genome Sequencing and Assembly

We obtained 104.3 Gb of PacBio long reads, with a mean read length of 15.42 Kb and an N50 length of 24.99 Kb. The genome was predicted to be between 395.5 and 397.2 Mb, with extremely low heterozygosity (Figure 2). We estimated that 31.22% of the assembly contained regions of repetitive sequences (Supplementary Table S1, Supplementary Material online). Our initial genome assembly, which was assembled solely from PacBio reads, was 371.791 Mb and contained 357 scaffolds and 1259 contigs (Table 1). We found that 93.9% of this assembly contained complete BUSCO genes (1,367), with a duplicate gene rate of 2.3% (Table 2). The mapping-back rates for Illumina short and PacBio long reads were 96.79% and 92.95%, respectively, which indicated that our assembly had high coverage of the raw data. There were approximately 800 Mb of Hi-C data used to assign

scaffolds and contigs onto the six chromosomes (Figures 3-4).

Genome Annotation

We annotated the repetitive sequences, protein-coding genes and non-coding RNAs from the genome assembly. There were 754,839 predicted repetitive sequences, which made-up approximately 116 Mb (31.22%) of the assembly. The five most abundant repeat types were DNA elements (11.64%), unclassified (10.72%), simple repeats (4.09%), LINEs (1.92%) and LTR elements (1.21%) (Supplementary Table S1, Supplementary Material online). There were 14,175 predicted protein-coding genes, supported by approximately 8 Gb of RNA-Seq data. The predicted genes had a mean length of 6,552.6 bp, a mean CDS length of 211.1 bp and a mean number of exons of 9.3 (Table 1). Of the genes that were completely recovered from this gene set, 93.9% were BUSCO genes. InterProScan identified protein domains for 11,227 predicted protein-coding genes and, together with eggNOG results, 9,607 and 8,287 genes were annotated with gene ontology (GO) terms and KEGG pathways, respectively.

We annotated 719 non-coding RNAs that contained 128 miRNAs, 89 rRNAs, 97 snRNAs, 225 tRNAs, 27 ribozymes, four lncRNAs and 149 other RNAs. The 97 snRNAs included 47 G4-forming RNAs (U1, U2, U4, U5, U6 and U11), three minor G4-forming RNAs (U4atac, U6atac and U12) and 47 C/D box snoRNAs (Supplementary table S2, Supplementary Material online).

Genome Collinearity Analysis

We found a relatively high level of conserved linkage between *N. formosana* (Nf) and *Acyrthosiphon pisum* (Ap) genomes, when compared with Nf and *Rhopalosiphum maidis* (Rm) genomes (Figure 5). *Neotoxoptera formosana* chromosome 1 (NfChr1) was mostly

collinear with ApChrX, with some small regions aligned to ApChrA2. We found that NfChr2 and NfChr6 had homologous regions on ApChrA1. The syntenic regions of NfChr3 were located on ApChrA1 and the entire of ApChrA3. Conservation was observed between NfChr4 and 5 and ApChrA2. When compared with the *R. maidis* genome, only NfChr1 showed a high level of conservation with RmChr3, whilst other chromosomes had syntenic regions scattered across the *R. maidis* genome.

Phylogeny

We used protein sequences from 15 species, together with the annotated *N. formosana* protein models, to construct a phylogenetic tree (Figure 6). There were 254,609 (91.3%) gene models assigned to 19,010 gene families. Among 4,169 gene families that were present in all species, 1,273 and 2,896 were single- and multi-copy families, respectively. In *N. formosana*, 14,037 genes were clustered into 9,838 families and 77 genes from 30 families were found to be specific to this species (Figure 6). A total of 555,217 amino acid residues, obtained from 1,113 single-copy genes, were used for phylogenetic construction. Most lineages had UFB/SH-aLRT supports of 100/100, apart from *Macrosiphini sacchari*, which had supports of 99.9/94, and *Aphis gossypii* and *Melanaphis sacchar*, which had supports of 99.3/98 (Figure 6). This phylogeny suggested that *N. formosana* and *Pentalonia nigronervosa* were sister groups.

Gene Family Evolution

When compared with the other species, we found that the number of expanded and contracted gene families in *N. formosana* was 629 and 3,067, respectively. There were 330 gene families

that showed significant expansion or contraction. The gene families with significant expansion were THAP domain, DDE superfamily endonuclease, zinc finger, immunity (ankyrin repeats), digestive enzyme (serine carboxypeptidase) and chemosensory receptor families (Figure. 7a). The Odorant receptors (ORs) gene family exhibited rapid expansion, in accordance with the GO enrichment analysis. The results of the KEGG pathway enrichment analysis showed that pathways involved in detoxification, immunity and secondary metabolite synthesis were significantly enriched (Figure 7b).

Aphid ORs play an essential role in the perception of different host odors or pheromones (Liu *et al.* 2022). In this study, 16 ORs candidate genes were rapidly exhibited expansion in *N. formosana*. This rapid expansion might be associated with the feeding behaviour of *N. formosana*, which is an oligophagic aphid pest only feeding on different *Allium* species. Hori (2007) finds that *N. formosana* might use dipropyl trisulphide (extracted from *Allium fistulosu*) and diallyl disulphide (extracted from *Allium tuberosum*) as olfactory cues to search for the host plants based on Y-tube olfactometer. In order to understand the odor perception of *N. formosana*, future work should analyze the expression patterns of ORs genes in different issues and identify the functional analysis of ORs genes to different plant volatiles (Zhang *et al*. 2019).

Data Availability

Genome assembly and raw sequencing data have been deposited at the NCBI under the accessions JAIWJD000000000 and SRR18085628, SRR18079676, SRR18079766 and SRR13334673, respectively. Genome annotations are available at the Figshare under the link: https://figshare.com/articles/online_resource/A_Chromosome-level_genome_assembly_of_Neotoxoptera_formosana_Takahashi_Takahashi_1921_Hemipte

ra_Aphididae_/19165817.

Acknowledgments

The authors are grateful to Prof. Feng Zhang and Mr Jian-Feng Jin (Nanjing Agricultural University, China) for their technical supports in data analysis. Bin-Xia Feng and Zhuo-Kun Liu (Guizhou University) were most helpful in rearing *Neotoxoptera formosana* populations.

Conflict of Interest

The authors declare that there is no conflict of interest.

Funding

This study was funding by the Provincial Key Technology Research and Development Program of Guizhou [2021(205)], Anshun City Science and Technology Plan Project ((2020)08), and the Natural Science Special Project of Guizhou University (Special post, [2020]-02).

Literature Cited

Asemani, Y., N. Zamani, M. Bayat, and Z. Amirghofran, 2019 *Allium* vegetables for possible future of cancer treatment. Phytother. Res. 33(12): 3019–3039.

Bao, W., K. K. Kojima, and O. Kohany, 2015 Repbase update, a database of repetitive elements in eukaryotic genomes. Mob. DNA 6(1): 1–6.

Brůna, T., A. Lomsadze, and M. Borodovsky, 2020 GeneMark-EP+: eukaryotic gene prediction with self-training in the space of genes and proteins. NAR Genom. Bioinform. 2(2): lqaa026.

284 Buchfink, B., C. Xie, and D. H. Huson, 2015 Fast and sensitive protein alignment using
285 DIAMOND. Nat. Methods 12(1): 59–60.
286 Bushnell, B. 2014 BBtools.Retrieved from: https://sourceforge.net/projects/ bbmap/.
287 Chan, P. P., and T. M. Lowe, 2019 tRNAscan-SE: searching for tRNA genes in genomic
288 sequences. Methods Mol. Biol. 1962:1–14.
289 Chen, C, H. Chen, Y. Zhang, H. R. Thomas, M. H. Frank, Y. He, and R. Xia, 2020 TBtools:
290 An integrative toolkit developed for interactive analyses of big biological data. Mol.
291 Plant. 13(8): 1194–1202.
292 Dudchenko, O., S. S. Batra, A. D. Omer, S. K. Nyquist, M. Hoeger, et al. 2017 De novo
293 assembly of the *Aedes aegypti* genome using Hi-C yields chromosome-length scaffolds.
294 Science 356(6333): 92–95.
295 Durand, N. C, M. S. Shamim, I. Machol, S. S. P. Rao, M. H. Huntley, et al., 2016 Juicer
296 provides a one-click system for analyzing loop-resolution Hi-C experiments. Cell. Syst.
297 3(1): 95–98.
298 Emms, D. M., S. Kelly, 2019 OrthoFinder: phylogenetic orthology inference for comparative
299 genomics. Genome Biol. 20(1): 238.
300 Flynn, J. M., R. Hubley, C. Goubert, J. Rosen, A. G. Clark, et al., 2020 RepeatModeler2 for
301 automated genomic discovery of transposable element families. Proc. Natl. Acad. Sci.
302 USA. 117(17): 9451–9457.
303 Guan, D, R. Hubley, C. Goubert, J. Rosen, A. G. Clark, et al. 2020 Identifying and removing
304 haplotypic duplication in primary genome assemblies. Bioinformatics 36(9):2896–2898.
305 Hoff, K. J., S. Lange, A. Lomsadze, M. Borodovsky, and M. Stanke, 2016 BRAKER1:
306 unsupervised RNA-seq-based genome annotation with GeneMark-ET and AUGUSTUS.
307 Bioinformatics 32(5): 767–769.
308 Holt, C, and M. Yandell, 2011 MAKER2: an annotation pipeline and genome-database
309 management tool for second-generation genome projects. BMC Bioinformatics 12(1):
310 491.
311 Hori, M., and H. Komatsu, 1997 Repellency of rosemary oil and its components against the
312 onion aphid, *Neotoxoptera formosana* (Takahashi) (Homoptera, Aphididae). Appl.
313 Entomol. Zool. 32(2): 303–310.

Horil, M., 2007 Onion aphid (*Neotoxoptera formosana*) attractants, in the headspace of *Allium fistulosum* and *A. tuberosum* leaves. J. Appl. Entomol. 131(1): 8–12.

Hu, J., J. Fan, Z. Sun, and S. Liu, 2020 NextPolish: a fast and efficient genome polishing tool for long read assembly. Bioinformatics 36(7): 2253–2255.

Huerta-Cepas, J., K. Forslund, L. P. Coelho, D. Szklarczyk, L. J. Jensen, et al., 2017 Fast genome-wide functional annotation through orthology assignment by eggNOG-mapper. Mol. Biol. Evol. 34(8): 2115–2122.

Huerta-Cepas, J., D. Szklarczyk, D. Heller, A. Hernández-Plaza, S. K. Forslund, et al., 2019 eggNOG 5.0: a hierarchical, functionally and phylogenetically annotated orthology resource based on 5090 organisms and 2502 viruses. Nucleic Acids Res. 47(D1): D309–D314.

Katoh, K., and D. M. Standley, 2013 MAFFT multiple sequence alignment software version 7: improvements in performance and usability. Mol. Biol. Evol. 30(4): 772–780.

Kim, D., J. M. Paggi, C. Park, C. Bennett, and S. L. Salzberg, 2019 Graph-based genome alignment and genotyping with HISAT2 and HISAT-genotype. Nat. Biotechnol. 37(8): 907–915.

Kovaka, S., A. V. Zimin, G. M. Pertea, R. Razaghi, S. L. Salzberg, et al. 2019 Transcriptome assembly from long-read RNA-seq alignments with StringTie2. Genome. Biol. 20(1): 278.

Kück, P., and G. C. Longo, 2014 FASconCAT-G: extensive functions for multiple sequence alignment preparations concerning phylogenetic studies. Front. Zool. 11(1): 81.

Li, H., 2018 Minimap2: pairwise alignment for nucleotide sequences. Bioinformatics 34(18): 3094–3100.

Li, H., B. Handsaker, A. Wysoker, T. Fennell, J. Ruan et al., 2009 The sequence alignment/map format and SAMtools. Bioinformatics 25(16): 2078–2079.

Lin, H. S., C. Zeng, H. Zhang, S. Zhang, J. Hu, et al., 2022 Identification of *Thrips alliorum* and insecticides screening for control it in field conditions. J. Mt. Agric. Biol. (In Press).

Liu, J., J. Xie, A. Khashaveh, J. Zhou, Y. Zhang, et al., 2022 Identification and tissue expression profiles of odorant receptor genes in the green peach aphid *Myzus persicae*. Insects, 13(5): 398.

Minh, B. Q., H. A. Schmidt, O. Chernomor, D. Schrempf, M. D. Woodhams, et al., 2020 IQ-TREE 2: new models and efficient methods for phylogenetic inference in the genomic era. Mol. Biol. Evol. 37(5): 1530–1534.

Quevillon, E., V. Silventoinen, S. Pillai, N. Harte, N. Mulder, et al., 2005 InterProScan: protein domains identifier. Nucleic Acids Res. 33, W116–W120.

Ruan, J., and H. Li, 2020 Fast and accurate long-read assembly with wtdbg2. Nat. Methods 17(2): 155–158.

Shahrajabian, M. H., W. Sun, and Q. Cheng, 2020 Chinese onion (*Allium chinense*), an evergreen vegetable: A brief review. Pol. J. Agron. 42: 40–45.

Smit, A. F. A., R. Hubley, P. Green, 2013–2015, RepeatMasker Open-4.0. Retrieved from: http://www.repeatmasker.org. Accessed June 7, 2020.

Song, Y. F., H. Zhang, C. Zeng, S. Ye, M.-F. Yang et al., 2021 Complete mitochondrial genome of *Neotoxoptera formosana* (Takahashi, 1921) (Hemiptera: Aphididae), with the phylogenetic analysis. Mitochondrial DNA PART B., 6(6): 1706–1707.

Stanke, M., R, Steinkamp, S. Waack, and B. Morgenstern, 2004 AUGUSTUS: a web server for gene finding in eukaryotes. Nucleic Acids Res. 32: W309–W312.

Steinegger, M., and J. Söding, 2017 MMseqs2 enables sensitive protein sequence searching for the analysis of massive data sets. Nat. Biotechnol. 35(11): 1026–1028.

Vurture, G. W., F. J. Sedlazeck, M. Nattestad, C. J. Underwood, H. Fang, et al. 2017. GenomeScope: fast reference-free genome profiling from short reads. Bioinformatics 33(14): 2202–2204.

Wang, X. H., Zhang, C. Zeng, C. Huang, S. Ye, et al. 2021 Predatory responses of *Aphidoletes aphidimyza* to *Neotoxoptera formosana*. Plant Protection 47(6): 128–133.

Waterhouse, R. M., M. Seppey, F. A. Simão, M. Manni, P. Ioannidis, et al. 2018 BUSCO applications from quality assessments to gene prediction and phylogenomics. Mol. Biol. Evol. 35(3): 543–548.

Yu, G., L.-G. Wang, Y. Han, and Q.-Y. He, 2012 clusterProfiler: an R package for comparing biological themes among gene clusters. Omics 16(5): 284–287.

Zhang, R. B., Y. Liu, S.-C. Yan, & G.-R. Wang, 2019 Identification and functional characterization of an odorant receptor in pea aphid, *Acyrthosiphon pisum*. Insect

science, 26(1): 58–67.

Table 1. Genome assembly statistics of *Neotoxoptera formosana*

Assembly	Total length (Mb)	Number of scaffolds	N50 length (Mb)	Longest scaffold (Mb)	GC (%)	BUSCO (n = 1,367) (%)			
						C	D	F	M
wtdbg	393.678	2,806	2.637	24.999	31.55	92.1	2.6	2.0	5.9
NextPolish	392.017	2,806	2.632	24.933	31.59	94.0	2.6	0.9	5.1
Purge_dups	376.840	1,911	2.800	24.933	31.15	94.0	2.6	0.9	5.1
3D-DNA	372.470	461	66.911	97.256	30.98	93.9	2.3	0.9	5.2
Final	371.791	357	66.908	97.223	30.96	93.9	2.3	0.9	5.2

Table 2. Genome assembly and annotation statistics for *Neotoxoptera formosana*.

	Neotoxoptera formosana
Genome assembly	
Assembly size (Mb)	371.791
Number of scaffolds/contigs	357/1,259
Longest scaffold/contig (Mb)	97.223/24.933
N50 scaffold/contig length (Mb)	66.908/2.772
GC (%)	30.96
Gaps (%)	0.024
BUSCO completeness (%)	93.9%
Gene annotation	
Protein-coding genes	14,175
Mean protein length (aa)	504.5
Mean gene length (bp)	6,552.6
Exons/introns per gene	9.3/8.0
Exon (%)	9.64
Mean exon length	271.4
Intron (%)	15.34
Mean intron length	501.4
BUSCO completeness (%)	93.9

Figure Legends

FIGURE 1. *Neotoxoptera formosana*. (A) *N. formosana* damaging *Allium tuberosum*; (B) *N. formosana* damaging yellow *A. tuberosum*; (C) *N. formosana* female and nymph.

FIGURE 2. The K-mer frequency distribution analysis of *Neotoxoptera formosana*.

FIGURE 3. Hi-C contact map of the *Neotoxoptera formosana* genome.

FIGURE 4. Circos plot that indicates chromosome length, GC content and protein-coding gene/repeat sequence density.

FIGURE 5. Chromosome collinearity analysis graph Ap: *Acyrthosiphon pisum*; Nf: *Neotoxoptera formosana*; Rm: *Rhopalosiphum maidis*.

FIGURE 6. Phylogenetic tree of *Neotoxoptera formosana*: The branch length represents evolution time, numbers represent the number of expanded, contracted and rapidly evolving (statistically significant, labeled as red) gene families in that branch.

FIGURE 7. Gene family evolution of *Neotoxoptera formosana*. (A) bubble plot of GO enrichment analysis of rapidly expanding gene families; (B) bubble plot of KEGG enrichment analysis of rapidly expanding gene families.

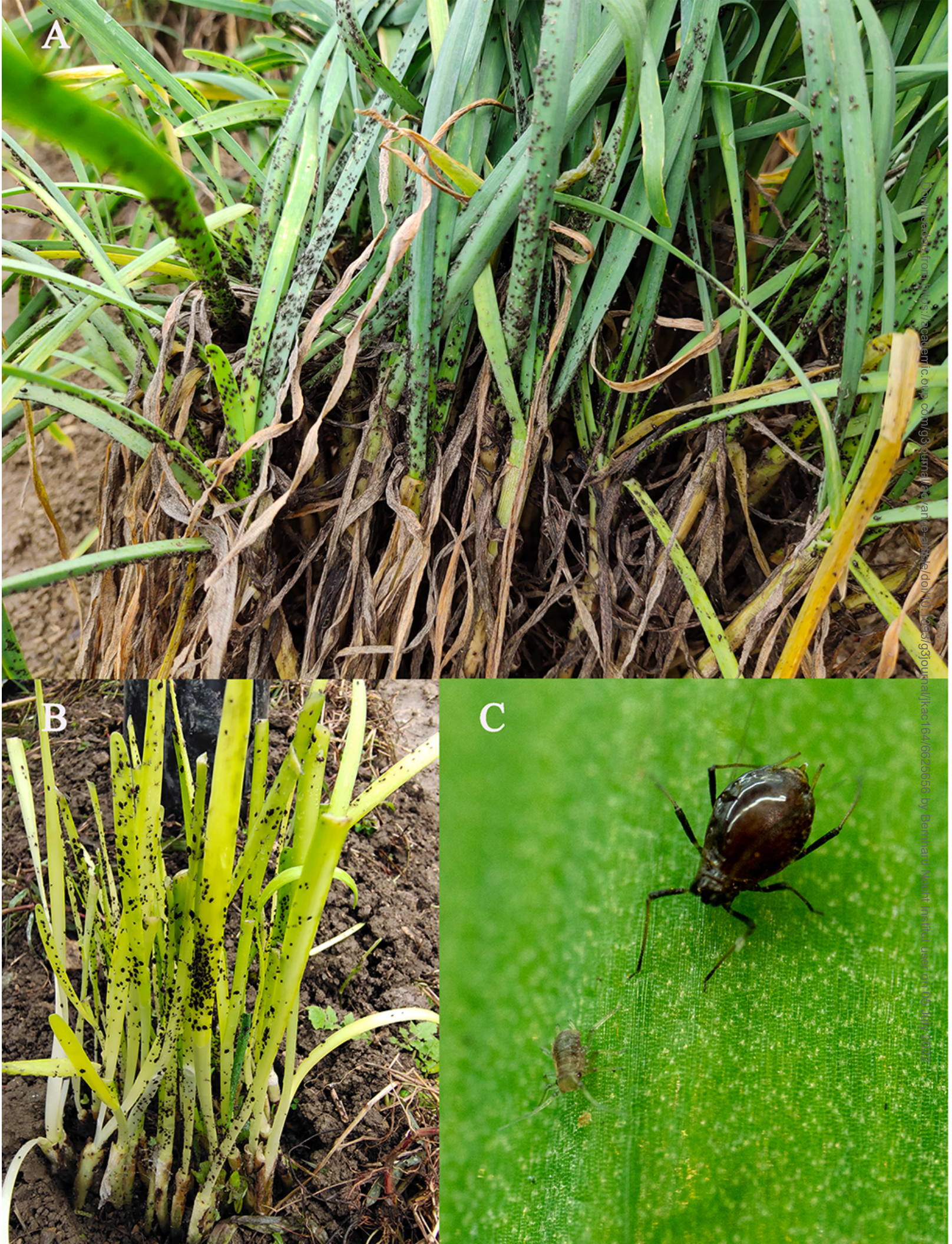
A
B
C